Experimental Investigation of Compression with Fixed-length Code Quantization for Convergent Access-Mobile Networks

L. Anet Neto[(1)], P. Chanclou[(1)], Z. Tayq[(1)], B. C. Zabada[(1)], F. Saliou[(1)], G. Simon[(1)]

[(1)] Orange Labs Networks, 2 Avenue Pierre Marzin, Lannion, France, luiz.anetneto@orange.com

Abstract *We experimentally assess compression with scalar and vector quantization for fixed-mobile convergent networks. We show that four-dimensional vector quantization allows 73% compression compliant with 3GPP EVM recommendations for transmissions over 25 km SSMF with 1:16 split ratio.*

Introduction

Animated discussions have been taking place recently on the convergence of fixed and mobile networks. It would allow operators to cope with increasing bit-rate demands while enabling infrastructure mutualisation and network consolidation. At the same time, it would provide clients seamless and flexible connection to the network thanks to the multiplicity of choices among the means to access different services[1].

Motivated by the massive deployment of fibre-to-the-premises (FTTx) on the one hand, ITU-T G.9807.1 symmetric 10 Gb/s passive optical network (XGS-PON) appears as an interesting alternative before the adoption of the second evolution of next-generation PON (NG-PON2). XGS-PON would allow an immediate and lower-cost solution capable of better accommodating mobile data traffic. Based on fixed-wavelength, time-division multiplexing (TDM), it could buy operators some time until tuneable transceivers become sufficiently mature for mass-production. Also, promising bandwidth allocation schemes have been reported to allow latencies compatible with mobile requirements while minimizing the wasted bandwidth associated to a PON user[2].

On the other hand, radio access networks (RAN) are currently evolving to embrace different features such as centralization, resource pooling and virtualization of some network functions. Those are perceived as key-enablers for flexible fifth generation (5G) mobile technologies with increased coverage and capacity. While previous mobile generations considered mainly backhaul fibre-based point-to-point (PtP) and potentially point-to-multipoint (PtMP) PON (Fig. 1a), the first RAN evolution (C-RAN) introduced centralization of the baseband units (BBU) thanks to a new, independent network segment known as fronthaul. The first fronthaul transmission deployment consists in most cases on fibre-based PtP connections from the BBU hotel, where all processing of the radio signals occurs (layers 1 to 3), to the remote radio heads (RRH) at the antenna sites. C-RAN evolution to provide higher capacity at the very short-term is based on low-cost, WDM solutions that allow fibre sharing[3] (Fig. 1b).

Transmission in the mobile fronthaul is often implemented using common public radio interface protocol (CPRI). Mobile signals are converted to non-return-to-zero (NRZ) sequences by means of pulse code modulation (PCM). This operation consists on sampling, quantizing and coding[4] the complex I/Q samples of the time-domain baseband mobile data. The NRZ symbols are then used to intensity modulate an optical carrier which is directly detected at the receiver-side before being reconverted back to the original mobile modulation format. Due to its binary nature, fronthaul transmissions are referred to as digital radio-over-fibre (D-RoF).

D-RoF benefited from the maturity of commercially available small-form factor pluggable transceivers used for optical metro/access applications. Also, since the signal is transmitted by means of ON/OFF keying, it provides extended robustness to optical noise and thus improved receiver sensitivities. However, its main drawback is its inherently poor spectral efficiency. For instance, in order to

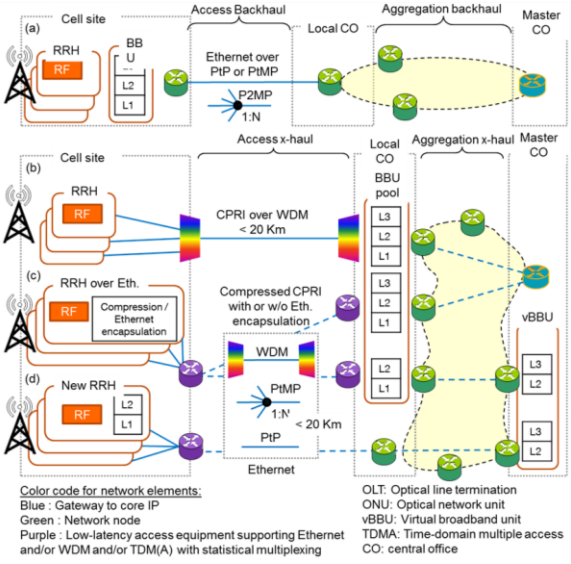

Fig. 1: (a) Existing mobile scenario, (b) CWDM C-RAN, (c) possible fixed-mobile convergent scenarios and (d) V-RAN.

transmit a 20 MHz downlink long-term evolution (LTE) signal in normal cyclic prefix mode, we would need a bit-rate of 1.2288 Gb/s in the optical link whereas the radio transmission itself would be limited to 100.8 Mb/s. Moreover, the fronthaul bit-rate scales with the number of sectors, frequencies, available technologies (2G/3G/4G) and antennas (with spatial diversity).

To allow the integration of mobile traffic into currently deployed and future PtMP TDM-based PON or simply to reduce the bit-rate constraints of nowadays PtP backhaul/fronthaul, it is thus essential to provide lower bit-rate D-RoF solutions. Reduced bit-rates would also reflect different functional splits in which, for instance, layer L1 and part of L2 are encapsulated into Ethernet frames. These are shown in Fig. 1c.

Here, we experimentally assess the impact of compression using different quantization techniques based on fixed-length coding. Our work is realized in the context of a short/mid-term evolution of the optical fronthaul, before the emergence of a fully virtualized convergent fixed-mobile network[5] (Fig. 1d). We assess currently adopted uniform quantization as well as non-uniform quantization using Lloyd's algorithm[6]. We also investigate multi-dimensional vector quantization with the Linde-Buzo-Gray (LBG) algorithm[7]. Using off-the-shelf SFP, we show that four-dimensional quantization allows 73% compression compliant with 3GPP error vector magnitude (EVM) recommendation after 25 km standard single mode fibre (SSMF) and with an 1:16 split ratio.

Experimental setup

Fig. 2 depicts our experimental setup. We generate a 20 MHz downlink (DL) LTE signal which is transformed using different quantization approaches. Quantization consists on converting the original signal samples into one of the 2^n possible levels of a finite-length set using the nearest neighbour condition, with n being the number of bits used by the quantizer. Then, a coder maps the indices of each of such levels into a NRZ word. A digital-to-analog converter (DAC) operating at 2 samples/symbol generates the analog NRZ signal used to modulate a directly modulated laser (DML) of a commercial SFP module emitting at 1510 nm

Tab. 1: OFDM LTE signal parameters.

Parameter	DL LTE signal	Our signal
Sampling freq. (MSa/s)	30.72	30.00
IFFT size	2048	2000
Occupied subcarriers	1200	1200
Null border subcarriers	847	799
CP size (samples)*	160 (5.21μs) | 144 (4,68μs)	160 (5.33μs) | 140 (4.67μs)
Useful symbol duration	66.67 μs	66.67 μs
Slot size (samples)	15360 (0.5ms)	15000 (0.5ms)
Subcarrier spacing (kHz)	15	15
Occupied BW (MHz)	18.015	18.015
FH bit-rate (Gb/s)**	1.2288	1.2000

* First | remaining 6 OFDM symbols of slot
** SISO, 15 bits/sample and 16/15*10/8 overhead[3]

and with 1 dBm mean optical power. The optical signal propagates through 25 km SSMF before being directly detected by an avalanche photodiode (APD). Extra 14 dB attenuation is added to emulate an 1:16 PtMP splitting-ratio. The bandwidth of the SFP is 3 GHz. The received NRZ signal is digitized with an analog-to-digital converter (ADC) working at 4 samples/symbol. Decision is taken on the received NRZ data to obtain the binary sequence used on the conversion back to the original LTE orthogonal frequency division multiplexing (OFDM) modulation. This is done using look-up-tables. In order to adapt the NRZ signal to the sampling characteristics of our ADC, we perform minor changes to some LTE PHY parameters, without loss of generality. Those are shown in Tab. 1. Finally, root mean square (RMS) EVM measurements are realized over 20 LTE slots (= 1 frame = 10 ms).

Results and discussions

Fig. 3 shows the impact on the received EVM when we vary the number of bits used to quantify each sample of the time-domain radio signal and thus the fronthaul bit-rate. The compression rate is defined using 15 bits quantization as reference. We consider the same number of quantization bits for all signal samples. Even if such solution provides lower performance compared to entropy-constrained quantization[8], it allows easier implementation.

In Fig.3, we compare two scalar (unidimensional) quantization solutions namely uniform quantization and non-uniform

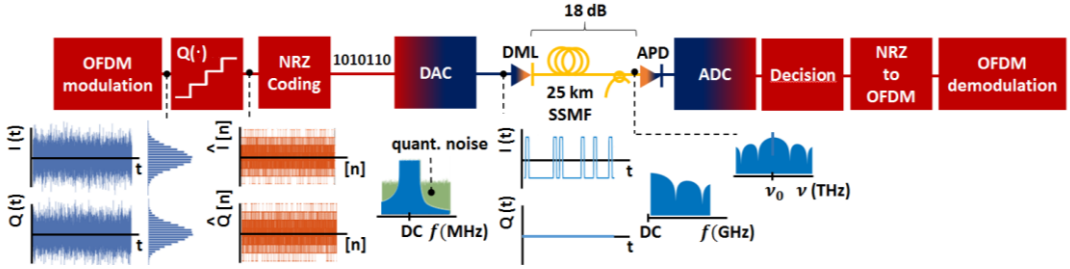

Fig. 2: Experimental setup.

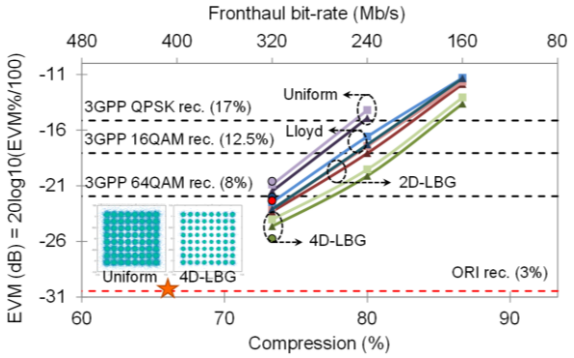

Fig. 3: EVM for different compressions and quantization techniques. 64QAM (●), 16QAM (■) and QPSK (▲).

quantization using the Lloyd algorithm. We also assess two vector quantization solutions using the LBG algorithm. We take I and Q dimensions for a two-dimensional (2D) vector quantization and separate each of them into odd and even indices samples for a four-dimensional (4D) solution. We should notice that for all compression rates tested in uniform mode, an optimal loading factor of 3σ was found to provide the best balance between overload and granularity quantization errors. Dynamic range adjustment is done on a LTE slot basis (0.5 ms).

From the central-limit theorem, we know that the probability density function (PDF) of the OFDM signal amplitude takes the form of a Gaussian distribution (insets of Fig. 2). Hence, uniform quantization cannot provide an optimal solution in our case. Lloyd's algorithm consists precisely on adapting the quantization levels to the PDF of the signal. It provides better precision (quantization levels closer together) on the amplitudes levels that have higher probability of being generated.

Fig. 4 (left) shows all possible combinations of quantization levels (circles) for independent non-uniform quantization in the I and Q components of the signal (points). It is clear that the corresponding mesh-grid (decisions thresholds of the quantization levels) does not provide an optimal sphere-packing solution. Indeed, it does not benefit from the correlation between I and Q samples of the OFDM signal happening due to the Fourier transform at the LTE modulator.

The LBG algorithm consists of an n-dimensional generalization of Lloyd's algorithm

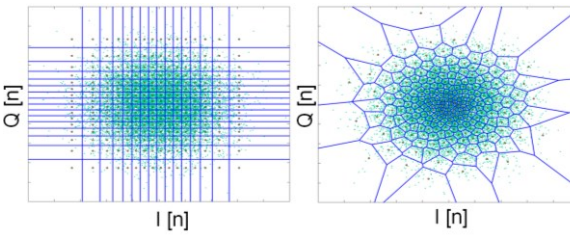

Fig. 4: 4 bits/sample comparison between scalar (left) and 2D vector quantization (right).

that allows benefiting from such statistical dependency and thus providing better EVM results, as shown in Fig. 3. The 2D-LBG solution shown in Fig. 4 (right) has an optimized arrangement of the quantization levels. The Voronoi cells represent the decision thresholds of each level. It is interesting to notice that I and Q samples of the time-domain OFDM signal also have some inner degree of correlation, which is why we implemented a four-dimensional LBG solution by separating the odd and even samples of the real and imaginary components of the signal.

4D-LBG allows a 4 dB gain in EVM with respect to uniform quantization, as shown in Fig. 3. Also, it enables compliance with 3GPP EVM recommendations with a compression rate of up to 73%. This corresponds to reducing the fronthaul bit-rate from 1.2 Gb/s to approximately 320 Mb/s in single-input single-output (SISO) mode. The received 64QAM constellations for uniform and 4D-LBG with 73% compression are show as insets in Fig. 3. We estimate that a 4D-LBG solution would allow up to approximately 67% compression (red star) compliant with Open Radio Interface (ORI) specification. We must notice that the achieved compression ratios could be further increased by means of cyclic prefix removal (6.67% of the slot duration) and low-pass filtering (LPF) allowing removal of unused border subcarriers[9]. As a reference, 4D-LBG would enable in this case up to 83% compression while keeping a 10% margin for the roll-off of the LPF.

Conclusions

We have experimentally assessed different quantization approaches for convergent fixed-mobile networks applications. Up to 73% bit-rate compression has been achieved with four-dimensional non-uniform quantization compliant with 3GPP EVM specifications after transmission over 25 km SSMF and a 1:16 split.

Acknowledgements

This work has been partially funded by the EU Horizon 2020 projects iCirrus (grant no. 644526) and 5G-PPP 5G-Crosshaul (grant no. 671598).

References

[1] J. Kani, W1H.1, OFC, 2016.
[2] T. Kobayashi et al., W3C.7, OFC, 2016.
[3] A. Pizzinat et al., J. Lightwave Technol., vol.33, no.5, pp.1077-1083,2015.
[4] A. Gersho, IEEE Trans. Circuits Syst, cas-25, no.7, 1978.
[5] K. Miyamoto et at., W1H.4, OFC 2016.
[6] K. Nieman and B. Evans, IEEE GlobalSIP, pp. 1198-1201, 2013.
[7] Y. Linde et al., IEEE Trans. Commun., vol.28, no.1, pp.84-95, 1980.
[8] H. Si et al., IEEE GLOBECOM, pp.1-6, 2015.
[9] B. Guo et. al, Bell Labs Tech. Journal, vol.18, no.2, pp.117-133, 2013.